Journal of Petroleum Exploration and Production Technology (2024) 14:2509–2527
https://doi.org/10.1007/s13202-024-01837-0

ORIGINAL PAPER - PRODUCTION ENGINEERING

Lattice Boltzmann simulation of cross-linked polymer gel injection in porous media

Elahe Kamel Targhi[1] · Mohammad Emami Niri[1] · Mohammad Reza Rasaei[1] · Pacelli L. J. Zitha[2]

Received: 26 May 2023 / Accepted: 15 June 2024 / Published online: 1 July 2024

Abstract

This study addresses the critical challenge of excessive water production in mature oil and gas reservoirs. It focuses on the effectiveness of polymer gel injection into porous media as a solution, with an emphasis on understanding its impact at the pore scale. A step-wise Lattice Boltzmann Method (LBM) is employed to simulate polymer gel injection into a 2D Berea sample, representing a realistic porous media. The non-Newtonian, time-dependent characteristics of polymer gel fluid necessitate this detailed pore-scale analysis. Validation of the simulation results is conducted at each procedural step. The study reveals that the methodology is successful in predicting the effect of polymer gel on reducing permeability as the gel was mainly formed in relatively larger pores, as it is desirable for controlling water cut. Mathematical model presented in this study accurately predicts permeability reductions up to 100% (complete blockage). In addition, simulations conducted over a wide range of gelation parameters, TD_factor from 1 to 1.14 and Threshold between 0.55 and 0.95, revealed a quadratic relationship between permeability reduction and these parameters. The result of this research indicates LBM can be considered as promising tool for investigating time-dependant fluids on porous media.

Keywords Lattice Boltzmann Method · Non-Newtonian fluid · Porous Media · Palabos · Computational Fluid Dynamics · Pore-scale modeling

Abbreviations

BGK	Bhatnagar-Gross-Krook
CEOR	Chemical Enhanced Oil Recovery
CFD	Computational Fluid Dynamics
CT	Computed Tomography (as in micro-CT image)
GLBM	Gray Lattice Boltzmann Method
LBM	Lattice Boltzmann Method
MPI	Message Passing Interface
MRT	Multiple Relaxation Time
SLBM	Simple Lattice Boltzmann Method
ULBM	Unstructured Lattice Boltzmann Method
WAG	Water Alternative Gas

Latin Letters

c_s	Sound speed of the lattice $\left(\frac{\text{LU}}{\text{TS}}\right)$
Cu	Carreau number
Dt	Time step (TS)
Dx	Lattice units in x direction (LU)
e_i	Discrete velocity
$\dot{e}$	Strain rate tensor
$e_{\alpha\beta}$	Local symmetric strain rate tensor
f_i	Distribution function
f_i^{eq}	Equilibrium distribution function
k	Permeability (LU^2)
l	Length of the flow domain (LU)
lx	Length of lattice unit in x direction (LU)
ly	Length of lattice unit in y direction (LU)
lz	Length of lattice unit in z direction (LU)
n	Power-law index for non-Newtonian fluid
N	Number of lattice units in each direction
Nx	Number of nodes in x direction
Ny	Number of nodes in y direction
Re	Reynolds number
TD_factor	Time-dependency factor in gelation process

✉ Elahe Kamel Targhi
kamelelahe@gmail.com

[1] Institute of Petroleum Engineering, School of Chemical Engineering, College of Engineering, University of Tehran, Tehran, Iran

[2] Department of Geoscience and Engineering, Delft University of Technology, Stevinweg 1, 2628 CN Delft, The Netherlands

Threshold	Critical relaxation frequency for gelation process
u	Velocity $\left(\frac{LU}{TS}\right)$

Greek letters

$\boldsymbol{\gamma}$	Shear rate (TS^{-1})
Δp	Pressure difference $\left(\frac{MU \times LU}{TS^2}\right)$
λ	Time constant (for calculating viscosity of non-Newtonian fluids)
ρ	Density $\left(\frac{MU}{LU^3}\right)$
ρ_{ref}	Reference density $\left(\frac{MU}{LU^3}\right)$
τ	Relaxation time (TS)
ν	Kinematic viscosity $\left(\frac{LU^2}{TS}\right)$
ν_0	Kinematic viscousity at zero shear-rate $\left(\frac{LU^2}{TS}\right)$
ν_∞	Kinematic viscousity at infinite shear-rate $\left(\frac{LU^2}{TS}\right)$
ω	Relaxation frequency (TS^{-1})
Ω_i	Collision operator
ω_0	Relaxation frequency at zero shear rate (TS^{-1})
ω_∞	Relaxation frequency at infinite shear rate (TS^{-1})

Introduction

The role of nonrenewable energy resources such as oil and gas in daily human life makes it necessary to use them efficiently (Hook et al. 2009). Unfortunately, the recovery factor from oil and gas reservoirs is significantly low, and many efforts have been made to enhance oil recoveries and increase production, such as polymer flooding, Low Salinity Water Flooding (LSWF), Chemical-Enhanced Oil Recovery (CEOR) and water alternative gas injection (WAG) (Bigdeli et al. 2023a; Bigdeli and Delshad 2023; Filho et al. 2023; Ghoreishi and Sedaee 2021; Hosseini-Nasab et al. 2016; Janssen et al. 2020). One of the most important problems facing oil and gas production is excessive water production, especially in mature reservoirs. The high amount of disposed water leads to high operating costs, including the cost of separation and damage to surface equipment, and the disposal of this water will cause many environmental problems (Bigdeli et al. 2023b; Mostafavi et al. 2021; Taha and Amani 2019). Most studies show that the main reason for the excessive water production is the existence of heterogeneity in high permeability ducts or thief zone (Bai et al. 2015). Therefore, by blocking high-permeability conduits, the flow paths are changed, resulting in producing oil from smaller pores and increasing the sweep efficiency (Dong et al. 2016).

Generally, various solutions have been proposed for the water shutoff (WSO), which fall into two main categories that can be used individually or in combination (Jiasheng 2013): Mechanical methods and chemical methods. Mechanical methods are generally concerned with using packers to seal the water excess zone (Liang and Zhang 2014). However, packers cannot penetrate the matrix or small fissures, so they are unable to shut off the excess water in some cases. Therefore, chemical methods, including the use of chemical solutions, are required in some cases. Polymer gel treatment is the most common method, among all the available solutions, due to its low price, good propagation in the reservoir, and easy opweation (Veliyev et al. 2019).

The use of polymer gel technology to reduce the amount of produced water had its beginning in the 1960s (Lashari et al. 2014). Polymer gel can flow through fractures, and it is also strong enough to tolerate high-pressure differences near the wellbore (Liao 2014). The combination of polymer and crosslinker is made ready on the surface, after which it is introduced into a production or injection well through injection. (Sydansk and Romero-Zerón, 2011). The less viscous solution has the ability to enter the channels with higher permeability, and once it reaches the point of gelation, it transforms into a solid-like gel. This gel aids in producing oil from areas that have not been swept previously (Taha and Amani 2019).

Injecting polymer gel deep into the reservoirs includes tons of complex fluid flow mechanisms. Also, fluid flow in porous media is one of the most important fields of study in petroleum engineering. The dynamics at the pore scale are controlled by capillary forces between the different fluid phases and the solid matrix (Golparvar et al. 2018). Because of various complex fluid flow mechanisms of polymer gel injection, it is necessary to understand the pore-scale description of the phenomenon to gain a better understanding of problems associated with oil gas oil reservoirs (Parmigiani et al. 2011).

For many decades, experimental studies were the only way to investigate fluid flow properties in porous media. Due to the complexity of performing experiments, specially on the pore scale (Yerramilli et al. 2015). Researchers tried to find a way to model mechanisms associated with the pore scale. While solving fluid flow problem using Navier–Stokes equations in a discretized domain often considered a promising tool in macroscopic scale, this method has a clear limitation in considering pore-scale pjenomenons as it ignores all the interations in moicroscopic scale and relies on the reservoir geometric properties such as porosity and saturation which can not be defined at pore-scale(Govindarajan 2019). Fully microscopic methds including Molecular Dynamics also becomes impractical for pore-scale simulations due to the immense number of molecules involved and consideration of full interactions leading to an exponential increase in computational demands that far exceed practical limits for such scale (Mollahosseini and Abdelrasoul

2021). On the other hand, mesoscopic methods including pore network modeling, smoothed particle hydrodynamics, and LBM can be considered good choice as they offer both the computational efficiency of macroscopic methods and the precision comparable to microscopic ones (Golparvar et al. 2018). Staring by Pore-network models, this method present a computationally less demanding alternative due to geometric simplifications, but it occasionallys overlook critical physical details, such as fractures in carbonate reservoirs, which can be pivotal in characterizing the reservoir's behavior (Blunt 2017; Ovaysi and Piri 2010). Smoothed particle hydrodynamics is a mesh-free, Lagrangian method that can handle complex free-surface flows but may be challenged by boundary conditions and consideration of inter-particle forces in this method also introduces substantial computational effort (Golparvar et al. 2018). So, according to the literature, the LBM is the most suitable method for modeling the injection of polymer gel thanks to its ability to model single and multiphase flows in complex geometries (Boek and Venturoli 2010; Martys and Chen 1996; Olson and Rothman 1997; Sukop et al. 2008) and its efficiency in terms of parallelization of the algorithm (Chen and Doolen 1998).

Although many efforts have been performed to experimentally simulate the injection of polymer gel, There are only few attempts to numerically simulate the flow of polymer gel in porous media at the pore scale (Al-Shajalee et al. 2020; Dong et al. 2016; Jia et al. 2011; Zheng et al. 2021; Zitha et al. 2002). In this study, we introduced the step-wise procedure to accurately simulate the injection of polymer gel in a two-dimensional segmented micro-CT image with the lattice Boltzmann method to investigate the changes in pore structure and permeability.

Lattice Boltzmann equation and BGK extension

The lattice Boltzmann method (LBM) was originally extracted from Lattice gas automata by replacing the boolean variable with a continuous distribution function (Chen and Doolen 1998). The evolution of the distribution function f_i is governed by the Lattice Boltzmann Equation (McNamara and Zanetti 1988) with the Bhatnagar, Gross, and Krook (BGK) approximation for the collision operator (Bhatnagar et al. 1954):

$$f_i\left(x+e_i,t+1\right)=f_i(x,t)-\frac{f_i-f_i^{eq}}{\tau}\quad(\mathrm{i}=1,2\ldots,M) \tag{1}$$

where f_i is distribution function, e_i is discrete velocity, and Ω_i is collision operator, τ is relaxation time, and f_i^{eq} is equilibrium distribution function. The Bhatnagar, Gross, and Krook (BGK) collision operator simplifies the complex interactions in the original collision term, making it suitable for modeling fluid flow at the mesoscopic level (Bhatnagar et al. 1954). This operator ensures that f_i relaxes to f_i^{eq} at a rate determined by τ, which is linked to the fluid's kinematic viscosity ν via the relation (Anbar et al. 2019):

$$\nu=\frac{2\tau-1}{6} \tag{2}$$

Modeling non-Newtonian flow with LBM

There are two common methods for simulating non-Newtonian fluid flow with the LBM in the literature. This section reviews key studies conducted using these approaches. Additionally, a summary of relevant research in this field is presented in Table 1.

Change relaxation time locally

Kinematic viscosity can be calculated from relaxation time. Therefore, one method for simulating non-Newtonian fluid flow involves calculating the relaxation time from viscosity. The first research in this field was conducted by Aharonov and Rothman (1993). They introduced a two-dimensional model for simulating non-Newtonian fluids in which relaxation time is calculated locally for each point at each time step, and their results matched with the power-law model perfectly.

Giraud et al. (1997) extended the classic lattice Boltzmann design for viscoelastic fluid with Chapman-Enskog and then investigated the models with Multiple Relaxation Times (MRT) (Giraud et al. 1998). After that, Lallemand et al. (2003) presented three-dimensional models with the help of the results of previous studies.

Boek et al. (2003) used the BGK model from the studies of Rakotomalala et al.(1996) and Aharonov and Rothman (1993) to investigate the flow of power-law fluid in the pipe and porous media, and their results have good agreement with analytical solution. Gabbanelli et al. (2005) examined this model for the truncated power-law model for both shear-thinning and shear-thickening fluids, observing a linear decrease in simulation error with increasing network resolution. After them, Kehrwald (2005) suggested that if the Cross model is used instead of the simple power-law model, much more accurate results will be obtained for complex fluids such as polyamides with in-situ polymerization.

In the field of non-Newtonian fluid flow in a porous medium, the first attempts by Sullivan et al. (2006) showed that these models could predict characteristics of the flow of non-Newtonian fluid in two-dimensional and three-dimensional porous media. They also suggested that the relationship between network resolution and simulation accuracy is a function of the power-law index.

Recently, Cristobal and Riera (2018) performed a detailed study on the modeling of non-Newtonian fluids with LBM.

Table 1 Summary of researches in the field of modeling non-Newtonian fluids with LBM

Model	Equation	References
Power-law	$\nu = k\lvert\gamma\rvert^{n-1}$	Aharonov and Rothman (1993), Boek et al. (2003), Boyd et al. (2006), Siddiki et al. (2018) and Sullivan et al. (2006)
Truncated power-law	$\nu = m\gamma_0^{(n-1)}, \quad \gamma < \gamma_0$ $\nu = m\gamma_0^{(n-1)}, \quad \gamma_0 < \gamma < \gamma_\infty$ $\nu = m\gamma_\infty^{(n-1)}, \quad \gamma_\infty < \gamma$	Afrouzi et al. (2019), Boyd and Buick (2007), Gabbanelli et al. (2005) and Siddiki et al. (2018)
Carreau-Yasuda	$\frac{\nu-\nu_\infty}{\nu_0-\nu_\infty} = \left[1+(\lambda\gamma)^a\right]^{\frac{n-1}{a}}$	Ashrafizaadeh and Bakhshaei (2009), Boyd and Buick (2007), Gokhale and Fernandes (2017) and Wang and Bernsdorf (2009)
Carreau	$\frac{\nu-\nu_\infty}{\nu_0-\nu_\infty} = \left[1+(\lambda\gamma)^2\right]^{\frac{n-1}{2}}$	Malaspinas et al. (2007) and Yoshino et al. (2007)
Cross	$\frac{\nu-\nu_\infty}{\nu_0-\nu_\infty} = 1+(\lambda\gamma)^{n-1}$	Kehrwald (2005)
Casson	$\mu = \begin{cases} \frac{\left(\sqrt{\tau_y}+\sqrt{\mu\lvert\dot{\gamma}\rvert}\right)^2}{\lvert\dot{\gamma}\rvert} & \tau > \tau y \\ \infty & \tau \le \tau_y \end{cases}$	Ashrafizaadeh and Bakhshaei (2009) and Ouared and Chopard (2005)
Herschel-Bulkley	$\mu = \begin{cases} \mu_0 & \lvert\gamma\rvert < \lvert\gamma_0\rvert \\ k\lvert\gamma\rvert^{n-1} + \tau_0\lvert\gamma\rvert^{-1} & \lvert\gamma\rvert > \lvert\gamma_0\rvert \end{cases}$	Wu et al. (2017)
Bingham	$\mu = \begin{cases} \frac{\tau-\tau_0}{\mu_\infty} & \tau > \tau_y \\ 0 & \tau < \tau_y \end{cases}$	Ginzburg (2002) and Tang et al. (2011)

They simulated different fluids to reach a steady-state in a channel and then analyzed the velocity profiles of Newtonian fluid and a non-Newtonian fluid using the Carreau model. Their study demonstrated the efficacy of LBM in simulating complex flows, including non-Newtonian fluids.

Despite the high accuracy of the methods presented using the BGK, these methods lose their accuracy when relaxation time approaches 0.5. For this reason, the researchers decided to model the non-Newtonian effect with MRT equations. Li et al. (2014), Grasinger et al. (2018), and Adam and Premnath (2019) have conducted the most significant researches in the development of the MRT models for non-Newtonian fluids. Also, considering this effect in other LBM schemes such as Gray Lattice Boltzmann Method (GLBM) (Chen et al. 2009), unstructured lattice Boltzmann method (ULBM) (Pontrelli et al. 2009), He-Luo incompressible lattice Boltzmann method (Tang et al. 2011), ILFVEA (hybrid of LBM and finite volume) (Zou et al. 2014), and Simple Lattice Boltzmann Method (SLBM) (Chen and Shu 2020) has also been examined.

It should be noted that because blood is the most well-known non-Newtonian fluid, extensive studies related non-Newtonian fluids have been conducted in this area of science (Afrouzi et al. 2019; Boyd et al. 2007; Ouared and Chopard 2005; Siddiki et al. 2018; Wang and Bernsdorf 2009).

Considering the non-Newtonian effect as a force of action

It has been proposed by some researchers that non-Newtonian behavior might be represented as an equivalent forcing effect. Accordingly, the non-Newtonian model typically comprises a Newtonian component coupled with an additional non-Newtonian effect, as indicated in the studies of Farnoush and Manzari (2014), Wang and Ho(2011) and Weiwei et al. (2019).

Methodology

Mathematical modeling

The modification of relaxation time in response to shear stress has been previously discussed as an effective method for modeling the shear dependency of non-Newtonian fluids. In this study, this method has been employed for numerical simulation. Additionally, the Carreau model has been chosen to represent the shear-dependency of the non-Newtonian fluid. For each time step, the step-wise procedure, which is also depicted in Fig. 1, is as follows (Sullivan et al. 2006):

1. Initiate all variables with an appropriate value. For example, if f_i (u = 0), the fluid is in a stationary state, and the effect of the applied force on the acceleration of the fluid motion is determined.

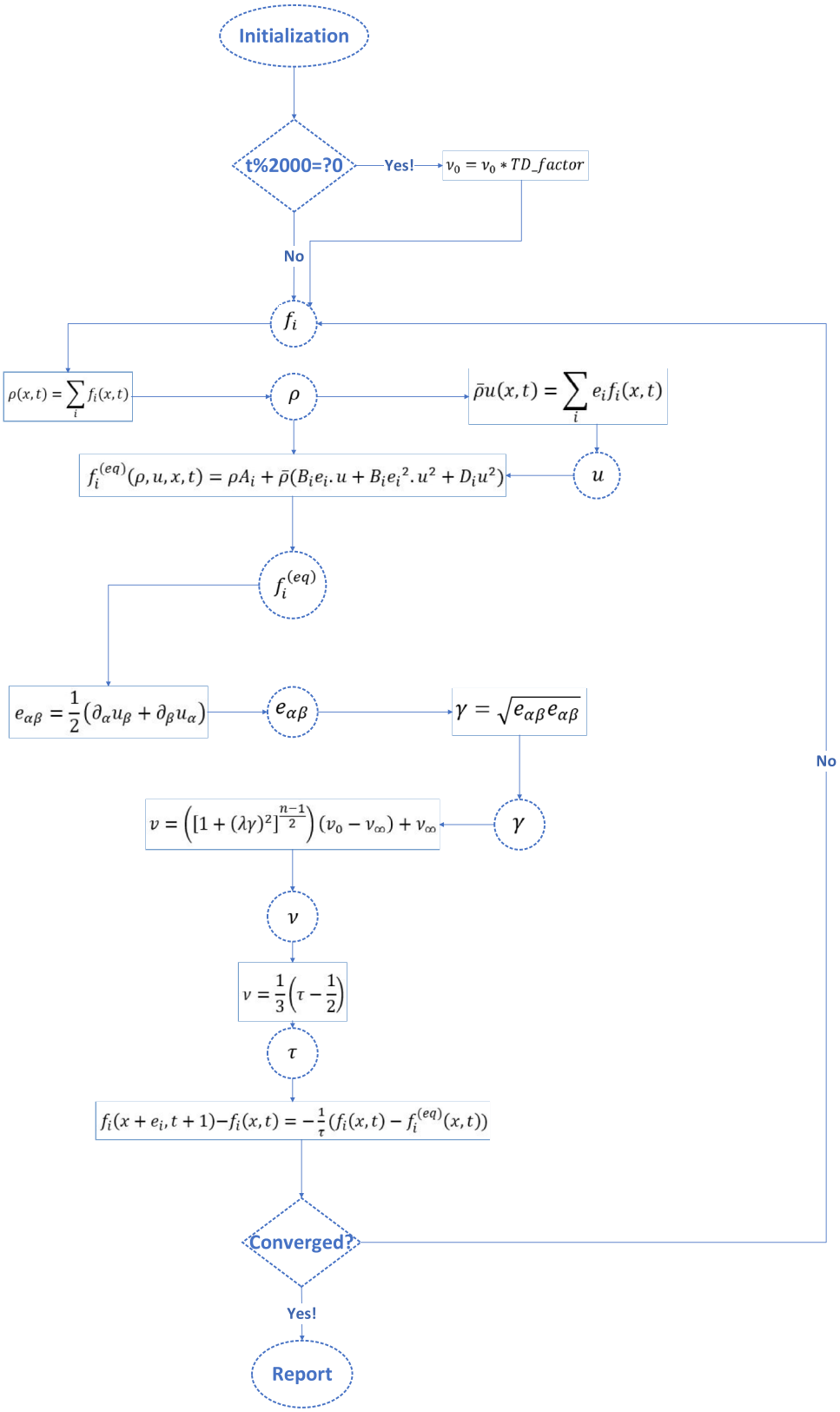

Fig. 1 Workflow for simulating shear dependent fluid with LBM for each time step t

2. Calculate the density (ρ) and fluid velocity (u) and then calculate the equilibrium distribution function $\left(f_i^{eq}\right)$.
3. Calculate the local symmetric strain rate tensor $\left(e_{\alpha\beta}\right)$ and then the strain rate tensor (ė)
4. Calculate kinematic viscosity (ν) from the Carreau model and obtain the relaxation time (τ)
5. Update the value of the distribution function $\left(f_i\right)$ at any point with the local value during the collision step
6. Perform streaming and transfer the distribution functions to the nearest neighbor node and also apply boundary conditions if necessary
7. Check the convergence condition, return to step 2 and repeat the steps until convergence is achieved

Given the advantages of Palabos (Parallel Lattice Boltzmann Solver) software, an open-source C++library developed specifically for computational fluid dynamics via the LBM, this platform has been chosen for the numerical simulations conducted in this study. Palabos is recognized for its efficiency in managing complex fluid dynamics scenarios and its ability to support a diverse range of models. The software effectively utilizes modern computing architectures, including parallel computing with MPI, facilitating high-performance simulations. This capability renders Palabos suitable for detailed academic research and practical i applications in fluid mechanics (Latt et al. 2021). Shear-dependency can be modeled perfectly in Palabos with the help of the fromPiAndRhoToOmega function, which is used to calculate ω $\left(\omega = \frac{1}{\tau}\right)$ of non-Newtonian fluid as below:

$$\omega = \frac{2}{1 + 2\left(\frac{\nu_0 - \nu_\infty}{c_s^2}\right)\left(1 + \alpha\omega_{iter-1}^2\right)^{\frac{n-1}{2}} + 2\frac{\nu_\infty}{c_s^2}} \tag{3}$$

where c_s is the sound speed of the lattice, ν_0 is fluid kinematic viscousity at zero shear-rate, ν_∞ is fluid kinematic viscousity at infinite shear-rate,ω_{iter} is relaxation frequency at iteration, and α is $\frac{1}{2}\frac{\gamma^2}{\left(\rho c_s^2\right)^2}$ which ρ is density.

Numerical simulation

The objective of this study is to simulate polymer gel injection in porous media, utilizing a two-dimensional segmented rock image obtained from micro-CT. To achieve this goal, the research process has been divided into smaller, more manageable steps, each of which is detailed in the subsequent sections.

Validating the non-Newtonian model

The mathematical model in Palabos software facilitates the modeling of Carreau fluid flow using the LBM. Prior to employing any CFD code for complex real-world phenomena, its validity must be verified. The purpose of this validation is to ensure the accuracy of the code in solving the implemented mathematical models with minimal error. Common examples employed for validating single-phase models, which have analytical solutions, include driven cavity flows, flow over a backward-facing step, Poiseuille flow inside a pipe, and flow around a circular cylinder. (Chen and Doolen 1998).

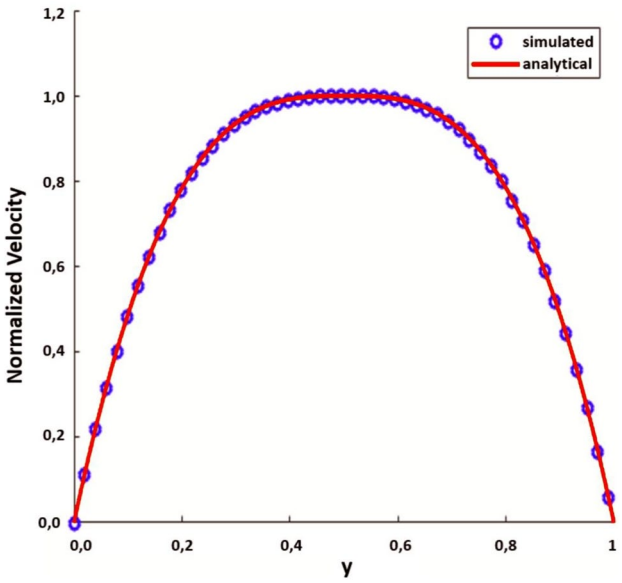

Fig. 2 Comparing the simulation result and analytical solution for normalized velocity profile of Poiseuille flow of non-Newtonian fluid of Table 1. The comparison shows an excellent match

Table 2 Input parameters for Poiseuille flow of Carreau fluid

Parameter	Definition	Value
u $\left(\frac{LU}{TS}\right)$	velocity	0.004951
Re	Reynolds number	1
Cu	Carreau number	10
N	Number of lattice units in each direction	101
lx (*LU*)	Length of lattice unit in x direction	1.00E+00
ly (*LU*)	Length of lattice unit in y direction	1
lz(*LU*)	Length of lattice unit in z direction	0.00E+00
dt (*TS*)	Time step	4.90E−05
n	Power-law index	0.5
ν_0 $\left(\frac{LU^2}{TS}\right)$	Kinematic viscosity at zero shear rate	5.00E−01
ν_∞ $\left(\frac{LU^2}{TS}\right)$	viscosity at infinite shear rate	0
ω_0	Relaxation frequency at zero shear rate	0.5
ω_∞	Relaxation frequency at infinite shear rate	2

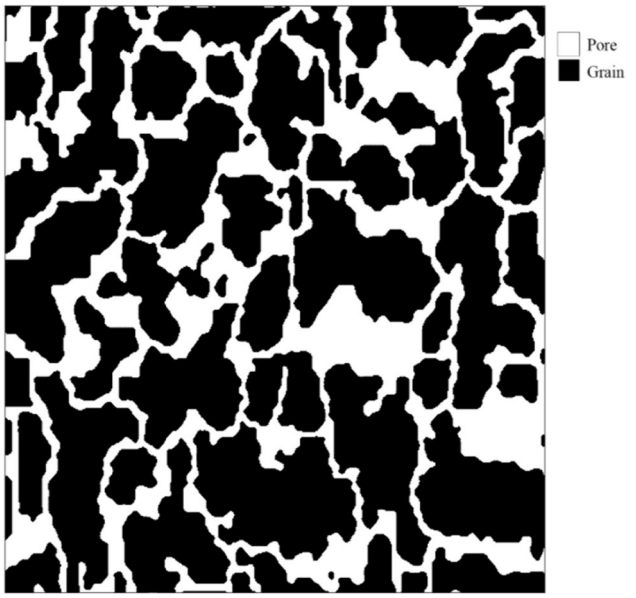

Fig. 3 Berea pattern used in the simulation. The grains are represented in black, and the pore spaces are in white. The size is 1418 µm by 1418 µm, and the etch depth of the physical unit is 24.54 µm (Boek and Venturoli 2010)

Validation of fluid flow in porous media

After the successful simulation of fluid flow in simple geometries, the accuracy of these simulations in more complex geometries must be examined. A 2D segmented image is utilized for this purpose. Prior to its use in Palabos, this image undergoes pre-processing. During this step, the segmented image is converted into a matrix with values 0, 1, and 2 using available MATLAB code. In this matrix, 0 and 2 represent the fluid and rock domains, respectively, while 1 denotes the interface between rock and fluid. Subsequently, the model's accuracy in predicting the flow of a Newtonian fluid in porous media is verified against available analytical solutions and relationships.

Simulation of polymer gel injection in a porous media

The code's ability to predict the behavior of shear-thinning fluids is evaluated by altering the power-law index and subsequently comparing the omega field and shear rate. Additionally, in fluids like polymer gel, where viscosity increases over time due to chemical reactions—a process known as gelation—this study models this phenomenon by varying the parameters of the non-Newtonian fluid model after several simulation steps. Specifically, the gelation process is represented by incrementing the value of ν_0. This increment is assumed to be linear over time and is achieved by multiplying ν_0 by a parameter termed the 'time dependency factor' (TD_factor) at selected time steps. Figure 1

Table 3 Input parameters and results of flow simulation of a Newtonian fluid in Berea sample

Parameter	1	2	3	4	5	6	7	8	9	10	11	12	13	14	15
Nx (LU)	400	400	400	400	400	400	400	400	400	400	400	400	400	400	400
Ny (LU)	400	400	400	400	400	400	400	400	400	400	400	400	400	400	400
$\Delta p\left(\frac{MU\times LU}{TS^2}\right)$	0.01	0.0075	0.005	0.0025	0.001	7.50E−04	5.00E−04	2.50E−04	1.00E−04	7.50E−05	5.00E−05	2.50E−05	1.00E−05	5.00E−06	2.50E−06
Re	2.51E+00	1.87E+00	1.24E+00	6.17E−01	2.46E−01	1.84E−01	1.23E−01	6.14E−02	2.46E−02	1.84E−02	1.23E−02	6.14E−03	2.46E−03	1.23E−03	6.14E−04
$v_0\left(\frac{LU^2}{TS}\right)$	0.2	0.2	0.2	0.2	0.2	0.2	0.2	0.2	0.2	0.2	0.2	0.2	0.2	0.2	0.2
$v_\infty \frac{LU^2}{TS}$	0	0	0	0	0	0	0	0	0	0	0	0	0	0	0
Cu	5	5	5	5	5	5	5	5	5	5	5	5	5	5	5
n	1	1	1	1	1	1	1	1	1	1	1	1	1	1	1
TD_factor	1	1	1	1	1	1	1	1	1	1	1	1	1	1	1
$u_{avg}\left(\frac{LU}{TS}\right)$	2.70E−05	1.98E−05	1.33E−05	6.74E−06	2.69E−06	2.01E−06	1.35E−06	6.75E−07	2.71E−07	2.01E−07	1.35E−07	6.77E−08	2.71E−08	1.35E−08	6.77E−09
$k\left(LU^2\right)$	0.216	0.215	0.215	0.214	0.214	0.214	0.214	0.214	0.214	0.214	0.214	0.214	0.214	0.214	0.214
$u_{avg}^{*}\nu^{*}1$	2.16E−03	1.58E−03	1.07E−03	5.39E−04	2.15E−04	1.61E−04	1.08E−04	5.40E−05	2.17E−05	1.61E−05	1.08E−05	5.41E−06	2.17E−06	1.08E−06	5.41E−07

includes the mathematical mpdeling for simulating behavior of polymer gel considering the increase in every 2000 timesteps. It is important to acknowledge that this methodology does not account for other factors that might influence viscosity, such as salinity and temperature. The focus of this initial stage in modeling polymer gel using LBM is solely on gelation.

Post-processing and observation of gelation:

In the post-processing stage of the simulation, it is essential to analyze the results to identify areas where gel formation occurs. A critical step involves defining a specific viscosity threshold for gelation, beyond which the fluid cannot move. Given the infinite viscosity in areas containing the rock matrix, working directly with the viscosity field presents challenges. Therefore, owing to the inverse relationship between relaxation frequency and viscosity, the relaxation frequency field is extracted from Palabos at the conclusion of the simulation. Subsequently, this field is post-processed using Python to discern structural changes. A parameter, referred to as 'Threshold' is designated to determine the minimum relaxation frequency allowing fluid movement. In regions where the relaxation frequency is lower than the Threshold, it is inferred that gel formation has blocked the pores. Consequently, the selected Threshold value has a direct impact on the change in permeability of the porous media following polymer gel injection.

Investigate changes in the geometry of the porous media and reduction of permeability:

In the subsequent stage, pores obstructed by gel formation are reclassified as part of the rock matrix. Consequently, the final output of this stage is a segmented image representing the rock's structure post-injection. This image is then further post-processed using MATLAB. Subsequently, the permeability of the altered pore structure is calculated using Palabos software. The variance between the initial permeability and the permeability post-injection quantifies the reduction in permeability attributable to the polymer gel injection.

Curve fitting and finding the best relationship between gelation parameters and permeability reduction:

In the final step, the study aims to ascertain if a mathematically sound relationship exists between the percentage of permeability reduction and the gelation parameters. For this purpose, the CFtool toolbox from MATLAB software is employed to examine various potential relationships and identify the most appropriate one.

Results and discussion

The outcomes of this study are detailed herein, building upon the methodologies outlined earlier. For further details on the computational methodology, the associated code is available in the authors' GitHub repository.[1]

Model validation of non-Newtonian fluid flow in simple geometry (Poiseuille)

A The initial step involves validating the model with an analytical solution. To this end, the Poiseuille flow of a non-Newtonian fluid is simulated and its results are compared with an analytical solution. This fundamental and straightforward flow type occurs in a pipe or between two parallel plates, as characterized by Sutera and Skalak (1993). Under these conditions, the velocity at the walls is zero (due to the non-slip condition), and the velocity reaches its maximum in the middle. The analytical solution for the flow of a non-Newtonian fluid in a pipe is as follows:

$$u(y) = \left(\frac{n}{n+1}\right)\left(\frac{\Delta p}{\rho_{ref} v_0}\right)\left[\left(\frac{H}{2}\right)^{\frac{n+1}{n}} - \left(\frac{H}{2} - y\right)^{\frac{n+1}{n}}\right] \quad (4)$$

where u is velocity, n is power-law index, Δp is pressure difference, ρ_{ref} is reference density, H is the width of the channel or pipe, and y shows the location where the velocity is calculated. As shown in Fig. 2, our model can accurately predict the behavior of the Carreau fluid of Table 2 in the pipe. It should be noted the input parameter in Table 2 are based on implementation of Poiseuille flow in Palabos software.

Verify the code for the flow of Newtonian fluid in porous media

It is necessary to verify the validity of the developed code in porous media simulations. Utilizing Darcy's law, the following relationship can be established:

$$u = -\frac{k}{\mu} \cdot \frac{\Delta p}{l} \quad (5)$$

[1] https://github.com/kamelelahe/NN-LBM.

Table 4 Simulation parameters and results of Newtonian, time-independent non-Newtonian, and time-dependent non-Newtonian fluids' motions in a 2D Berea sample

	Number	Parameter	Newtonian	Polymer	Polymer gel
Porous media properties	1	N	400	400	400
	2	lx	*1*	1	1
	3	ly	1	1	1
	4	lz	0	0	0
	5	Dx (LU)	0.0025	0.0025	0.0025
	6	Dt (TS)	1.54E−07	1.54E−07	1.54E−07
	7	Nx	400	400	400
	8	Ny	400	400	400
Flow properties	9	U $\left(\frac{LU}{TS}\right)$	6.15E−05	6.15E−05	6.15E−05
	10	Re	0.12	0.12	0.12
	11	deltaP $\left(\frac{MU\times LU}{TS^2}\right)$	0.0005	0.0005	0.0005
Non-Newtonian fluid properties	12	Cu	5	5	5
	13	n	1	0.8	0.8
	14	Nu0 $\left(\frac{LU^2}{TS}\right)$	0.2	0.2	0.2
	15	NuInf $\left(\frac{LU^2}{TS}\right)$	0	0	0
	16	Omega0	0.91	0.91	0.91
	17	OmegaInf	2	2	2
	18	lambda	3.25E+07	3.25E+07	3.25E+07
Gelation parameters	19	Threshold	0.75	0.75	0.75
	20	TDfactor	1	1	1.11
Results	21	porosity	0.33	0.33	0.20
	22	Perm (LU^2)	0.21	0.21	0.02
	23	Porosity reduction (%)	0	0	45.12
	24	Perm reduction (%)	0	0	93.43

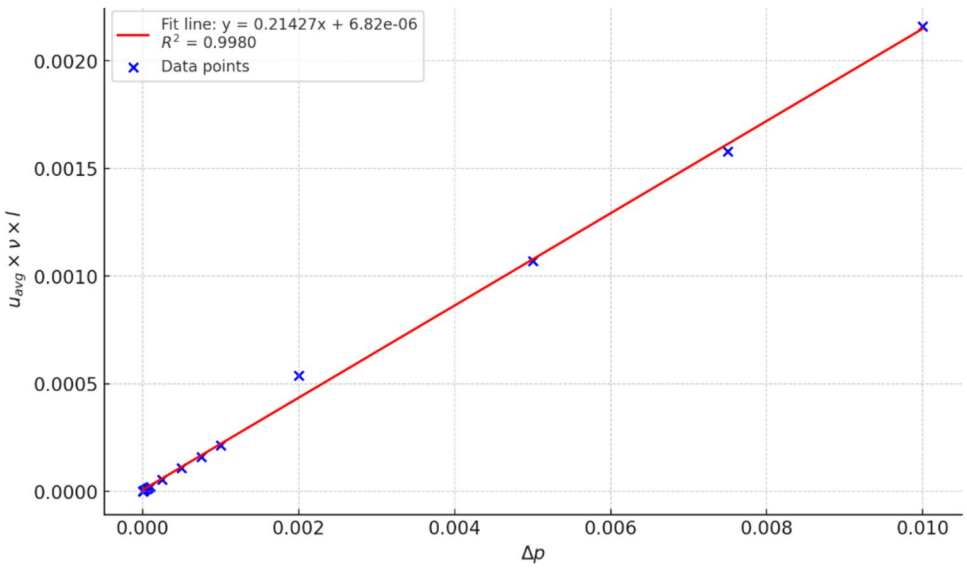

Fig. 4 Validation of flow of Newtonian fluid in 2D Berea sample. The slope of this plot indicates permeability

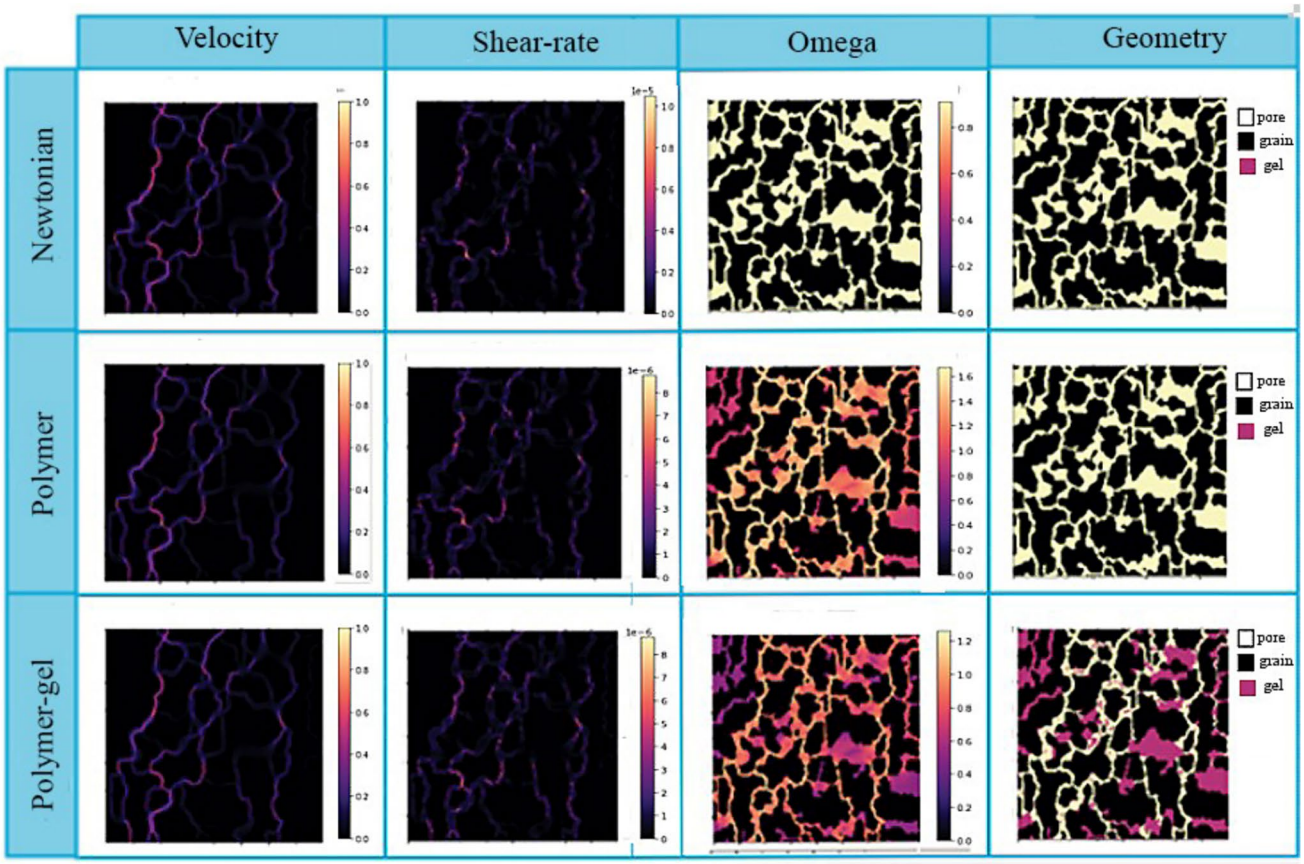

Fig. 5 Velocity field, shear-rate, omega, and geometry changes after injecting different types of fluids in a 2D Berea sample

where u is velocity, k is permeability, μ is viscosity, Δp is pressure difference, and l is the length of the flow domain. Based on the formula, there is a linear relationship with the slop of permeability between velocity and $\frac{\Delta p}{\mu * l}$. arious simulations were conducted by altering Δp to investigate this relationship furthur. The geometry of the porous media for these simulations utilized a square cross-section of the two-dimensional Berea micro-model, as proposed by Boek and Venturoli (2010), and is depicted in Fig. 3. The boundary conditions implemented were constant pressure (Zou and He 1995) at the inlet and outlet (on the right and left sides, respectively), with a bounce-back scheme applied at the interface between the rock and fluid domains. The input parameters and the results of these simulations are presented in Table 3. As demonstrated in Fig. 4, the results exhibit a strong correlation with a slope of approximately 0.214, which is in agreement with the permeability estimated by the code.

Simulation of polymer gel injection in porous media and investigate the changes in geometry

After successfully validating the code, we can now use it for simulating the injection of polymer gel in porous media. The value of ν_0 was increased at every 2000 iterations to mitigate the risk of divergence. The values for TD_factor and Threshold could be methodically chosen to reflect a desired of gelation behaviors within porous media, allowing the simulation to adapt to a variety of potential real-world gelation scenarios. This non-specific selection is intended to provide a versatile modeling approach rather than to replicate the behavior of any particular polymer gel.

In this phase of research, simulations were conducted for three fluid types with differing rheological properties: a Newtonian fluid, a shear-thinning polymer, and a shear-thinning, time-thickening polymer gel. The input parameters and results for these fluids are detailed in Table 4. The results, illustrated in Fig. 5, show that while the omega field remains constant for the Newtonian fluid, indicating uniform viscosity, it varies for the non-Newtonian fluids, displaying elevated values in regions of higher velocity or shear rate, notably within smaller pores.

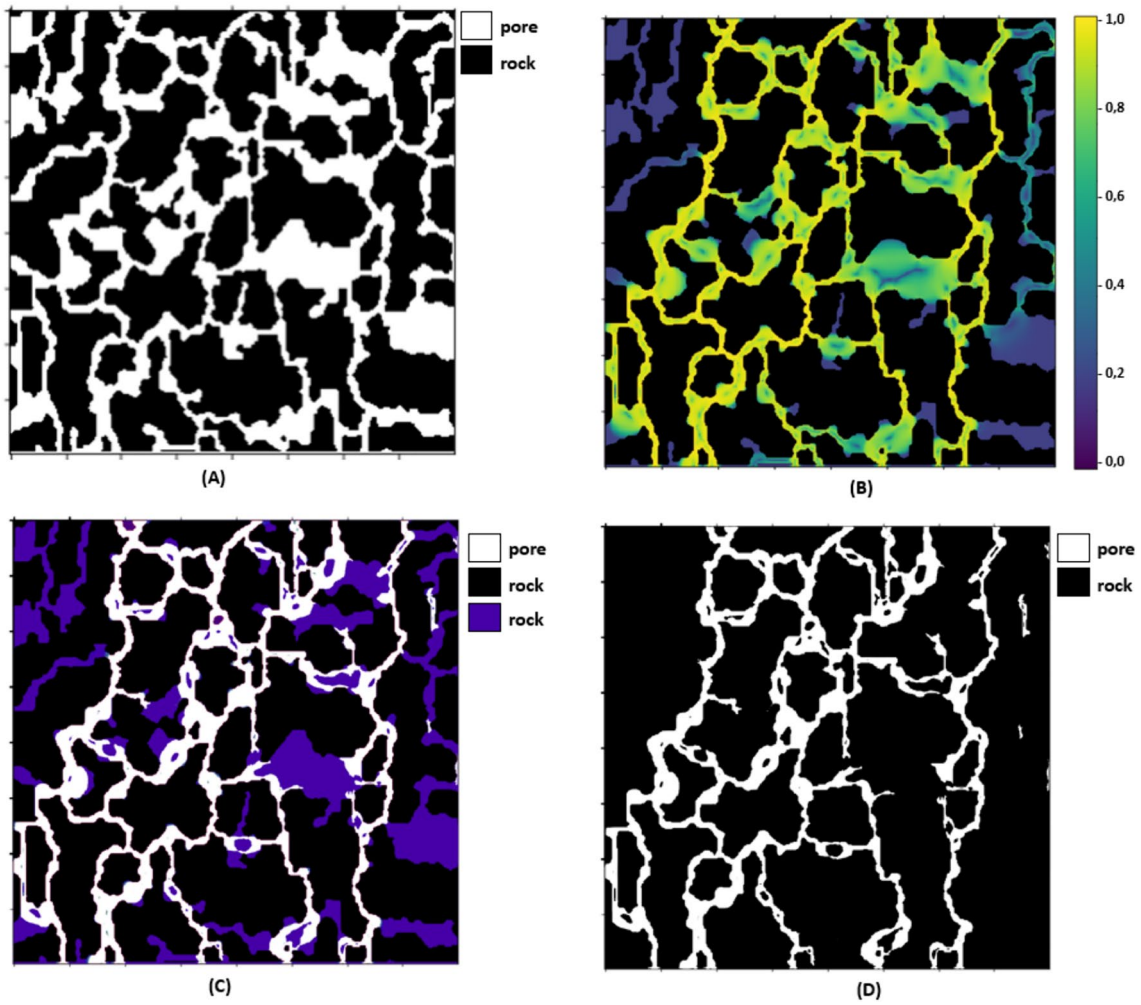

Fig. 6 Schematic of different stages of the simulation. **A** Initial rock geometry, **B** relaxation frequency field at the end simulation, **C** formation of gel in pores, **D** rock geometry after injection of polymer gel

Furthermore, analysis of the rock geometry post-simulation reveals that the gel formation process is accurately represented in the polymer gel simulation, with no significant geometrical change observed for the Newtonian fluid and polymer simulations. The segmented images suggest that gel predominantly forms in comparatively larger pore spaces, as visually discernible from the micro-CT images, supporting the simulation's validity. This outcome aligns with the objective of polymer gel injection strategies, which aim to obstruct more permeable pathways to enhance oil recovery from less permeable regions.To take a closer look, Fig. 6 summarizes the simulation procedure stages. This figure also indicated that polymer gel had changed the structure of porous media desirably.

Uderscoring relationship between gelation parameters and permeability reduction

In this section, efforts are made to derive a mathematical relationship linking gelation threshold and TD_factor with permeability reduction. It is important to note that the results pertain specifically to the selected range of parameters. The primary aim here is to demonstrate the simulator's ability to capture the gelation phenomenon within this defined parameter space.

Effect of gelation threshold

Two parameters in this study have been identified as critical in defining the gelation behavior. The influence of the gelation threshold on the alteration of the porous media structure and the subsequent reduction in permeability is the focus of this section. By utilizing the omega field

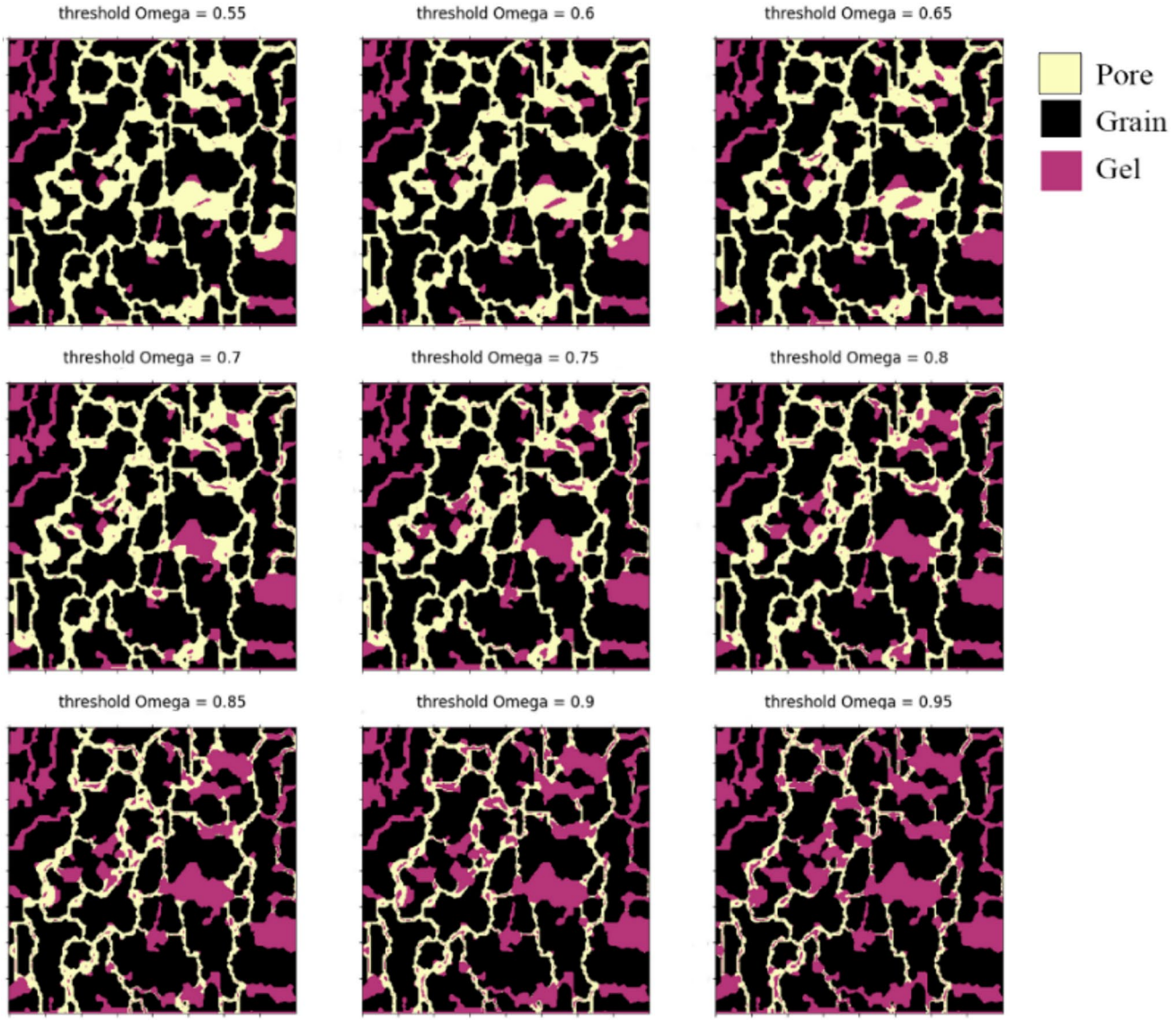

Fig. 7 Formation of gel with different threshold values in the pores of the Berea sample

data at the result of the polymer-gel fluid simulation (presented in Table 4) different threshold values were chosen to isolate only the effect of gelation threshold on permeability reduction. Figure 7 illustrates gel formation using threshold values that are varied from 0.55 (corresponding to ν_threshold = 0.44) to 0.95 (ν_threshold = 0.18). As can be seen, an increase in the threshold value results in an increased number of pores obstructed by the polymer gel. Elevating the maximum omega value, where polymer gel remains mobile within the pores, leads to a decrease in the minimum viscosity necessary for gel formation. Consequently, a larger number of pores satisfy the criteria for gel development.

The study subsequently explored the mathematical relationship between the Threshold value and permeability reduction. For each simulation conducted with a TD_factor ranging from 1.08 to 1.13, the Threshold was adjusted between 0.55 and 0.9. The percentage of permeability reduction was plotted to determine the best-fitting curve. As demonstrated in Fig. 8, a quadratic equation appears to accurately depict the relationship between permeability reduction and the Threshold. The derived overall equation is as follows:

$$y = ax^2 + bx + c \tag{6}$$

where x is Threshold and y is the percentage of permeability reduction. The coefficients for this relationship and some metrics for evaluating the goodness of the results are

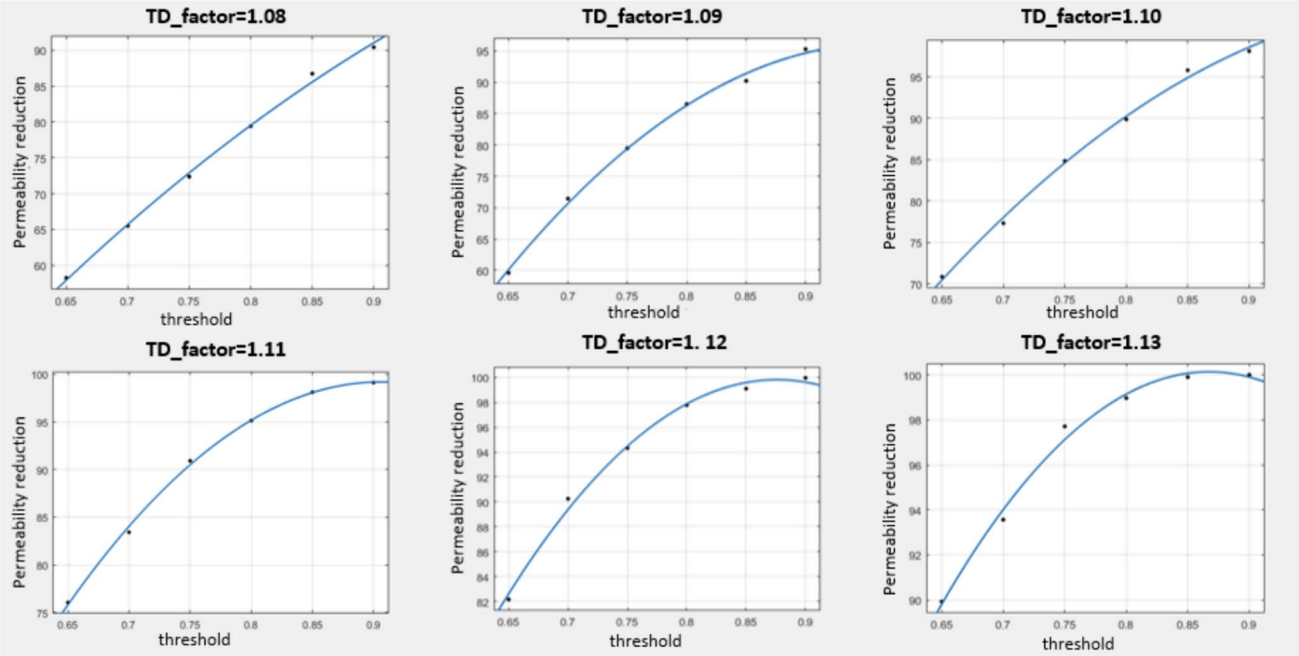

Fig. 8 Permeability reduction versus Threshold for different values of TD_factor. The simulation results are represented as dots, and the fitted quadratic equation is shown with a blue line

Table 5 Coefficients and metrics for the quadratic relationship between permeability reduction and threshold value for different TD_factor

TD	a	b	c	SSE	R-square	Adj R-sq	RMSE
1.08	− 115.3	311.1	− 95.57	2.17	1.00	1.00	0.85
1.09	− 395.2	704.3	− 243.4	2.66	1.00	0.99	0.94
1.1	− 193.9	413	− 116	1.88	1.00	0.99	0.79
1.11	− 356.2	645.5	− 193.3	0.63	1.00	1.00	0.46
1.12	− 336.6	589.7	− 158.5	1.34	0.99	0.99	0.67
1.13	− 218.2	378.6	− 64.08	0.62	0.99	0.99	0.46
Avg	− 269.23	507.03	− 145.14	1.55	1.00	0.99	0.70

presented in Table 5. Also, the residual plot for the quadratic equation is shown in Fig. 9.

Effect of TD_factor

Another important parameter that has a considerable impact on the formation of gel is TD_factor. For the purpose of this investigation, the TD_factor for the polymer-gel fluid was varied from 1 to 1.15. To isolate the impact of the TD_factor on the pore structure, a constant threshold value of 0.75 (corresponding to ν_threshold = 0.28) was selected for analysis. This particular value was chosen as a representative example to clearly delineate the sole effects of the TD_factor variation. The findings, as illustrated in Fig. 10, indicate that an increase in the TD_factor enhances the time-thickening behavior, leading to a higher viscosity and resulting in the obstruction of a greater number of pores by the polymer gel.

Again a mathematical representation for changing permeability reduction with TD_factor is investigated. For each threshold value between 0.65 and 0.9, we selected different values for TD_factor between 1.08 and 1.14. As it could be understood from Fig. 11, a quadratic equation similar to Eq. 6 with x as TD_factor seems to fit the data very well. The coefficients and metrics for the quadratic representation are reported in Table 6, and the residual plots are depicted in Fig. 12.

A general relationship between TD_factor, threshold, and permeability reduction

Analytical correlation for estimation of permeability reduction from gelation parameters is elaborated here. Using the generated simulation results, a two-variable equation between permeability reduction with the TD_factor has

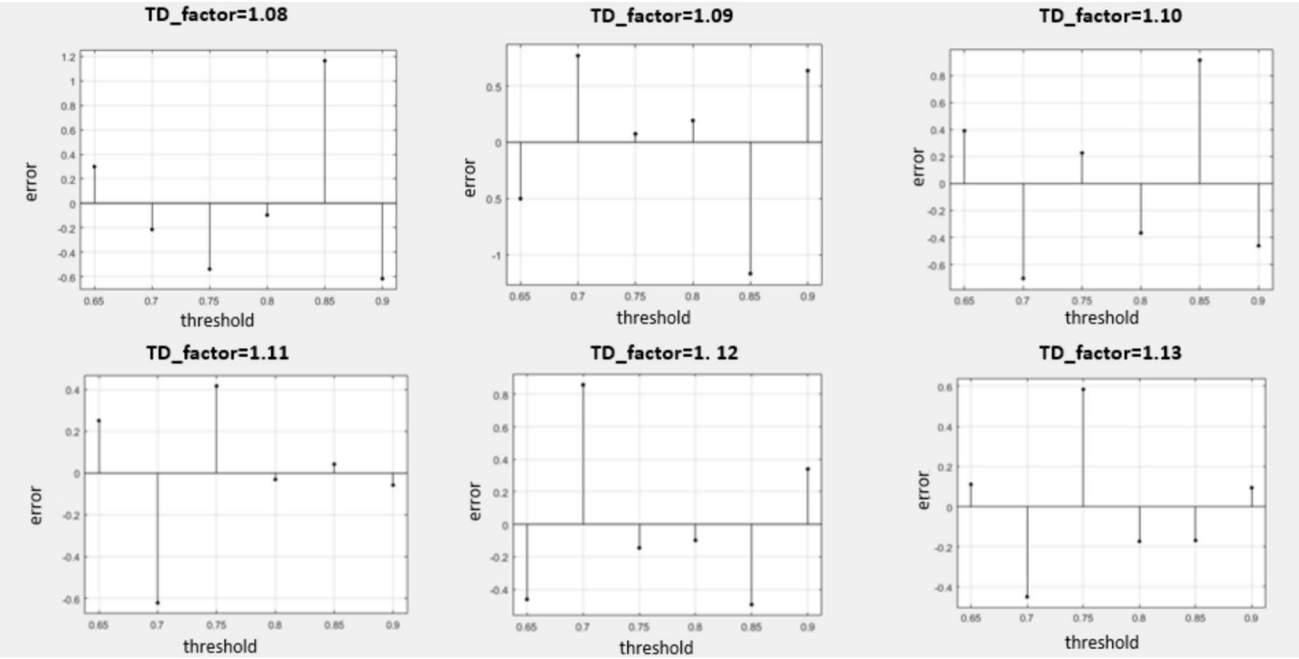

Fig. 9 Residual plot for the quadratic relationship between permeability reduction and Threshold for different values of TD_factor

been developed (between 1.08 and 1.14) and the gelation threshold (between 0.65 and 0.9). The selected range for the TD_factor and the gelation threshold is specifically designed to encompass gelation effects rather than scenarios without

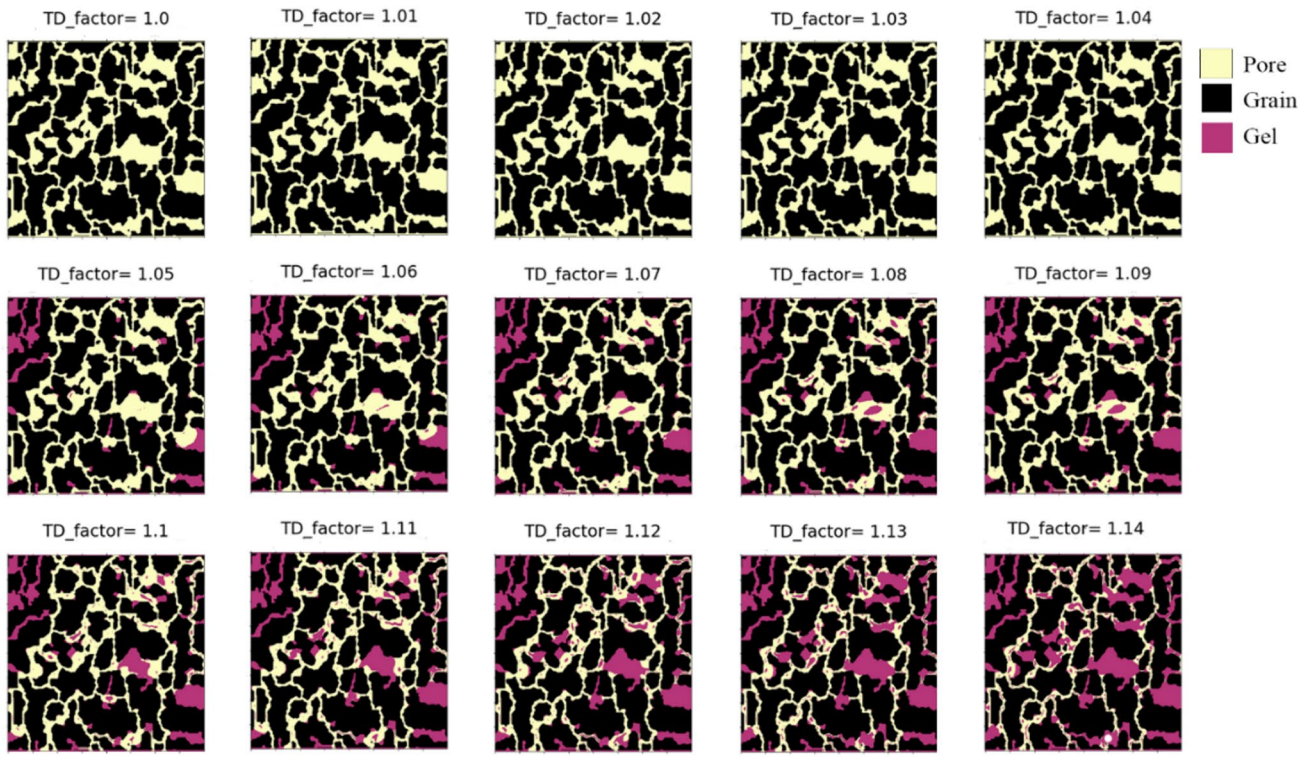

Fig. 10 Formation of gel in the pores of the Berea sample with different values for TD_factor

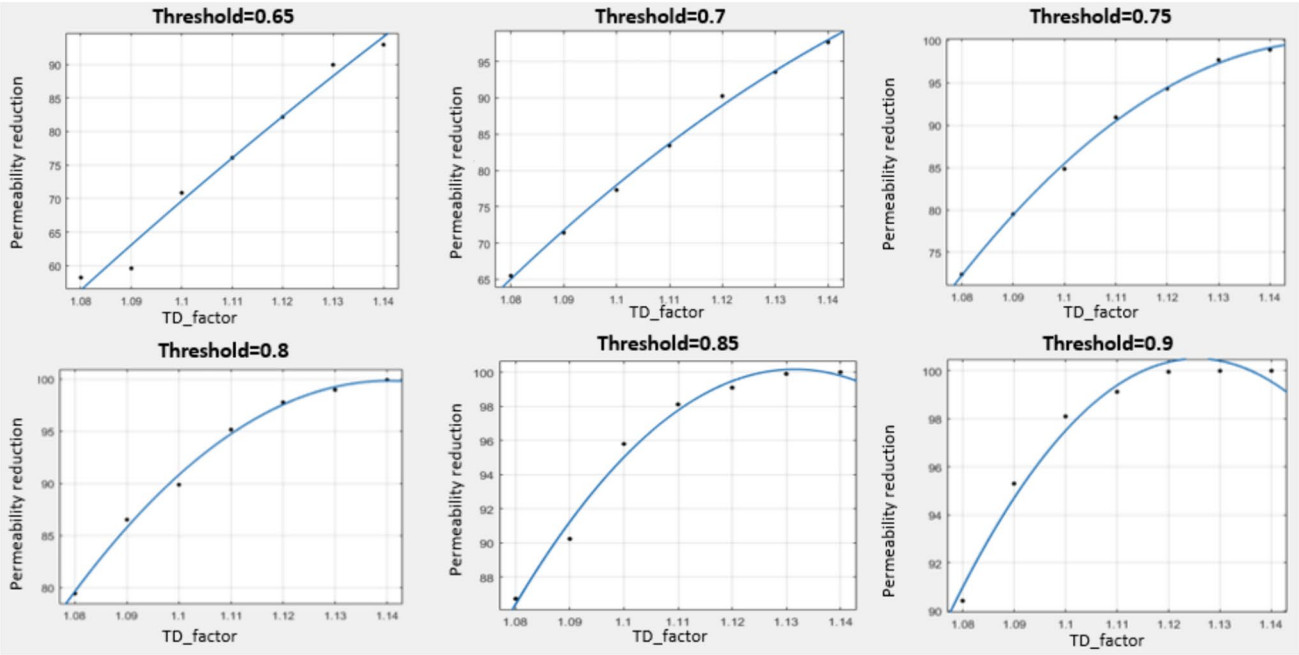

Fig. 11 Permeability reduction versus TD_factor for different values of Threshold. The simulation results are represented as dots, and the fitted quadratic equation is shown with a blue line

gel formation. As demonstrated in Fig. 12, a quadratic equation succinctly encapsulates this relationship, offering a predictive formula for the observed data.

$$f(x,y) = p00 + p10{*}x + p01{*}y + p20{*}x^2 + p11{*}x{*}y + p02{*}y^2 \quad (7)$$

where x is TD_factor, y is Threshold, and z is the percentage of permeability reduction. Table 7 and Fig. 13 show the coefficients and metrics of Eq. 7 and the residual plot for this curve, respectively.

Limitations and areas of improvement

The results obtained suggest that utilizing LBM to model polymer gel flow in porous media is a viable step forward. Given the nascent stage of research in this domain, the model incorporates certain simplifications. An isotropic porous medium is assumed, where transport properties such as permeability and porosity are considered uniform in all directions. Morover,the gelation threshold is considered as a fixed value depending the properties of porous media, and this limitation can be address in future works by calculating the drag force on the fluid and delineating gelation areas where the drag force is insufficient to mobilize the viscous fluid.

It is also to be noted that the mathematical model has been employed to generate a dataset for the development of an Artificial Neural Network(Kamel Targhi et al. 2023). This network is designed to estimate the effects of polymer gel injection using the model's input parameters. In adddtion, result of assessing the model in Kamel Targhi et al., (2023). is consistent with mathematical analysis over this paper, as it was concluded the TD_factor and threshold parameters have the most segnificat (Fig. 14).

Conclusions

According to the relative importance of polymer gel injection as a successful method for water shutoff treatment in oil and gas reservoirs, it is necessary to engineer this process

Table 6 Coefficients and metrics for the quadratic relationship between permeability reduction and TD_factor for different threshold values

Threshold	a	b	c	SSE	R-square	Adj R-sq	RMSE
0.65	590.9	−597.6	−0.29	21.33	0.98	0.97	2.31
0.7	216	−219.4	−0.87	2.62	1.00	1.00	0.81
0.75	129.6	−135.3	−1.01	0.83	1.00	1.00	0.45
0.8	114.8	−120.8	−1.04	1.78	0.99	0.99	0.67
0.85	107.7	−113.9	−1.05	2.08	0.99	0.98	0.72
0.9	102.5	−109.6	−1.07	1.64	0.98	0.97	0.64
Avg	210.25	−216.10	−0.89	5.05	0.99	0.99	0.93

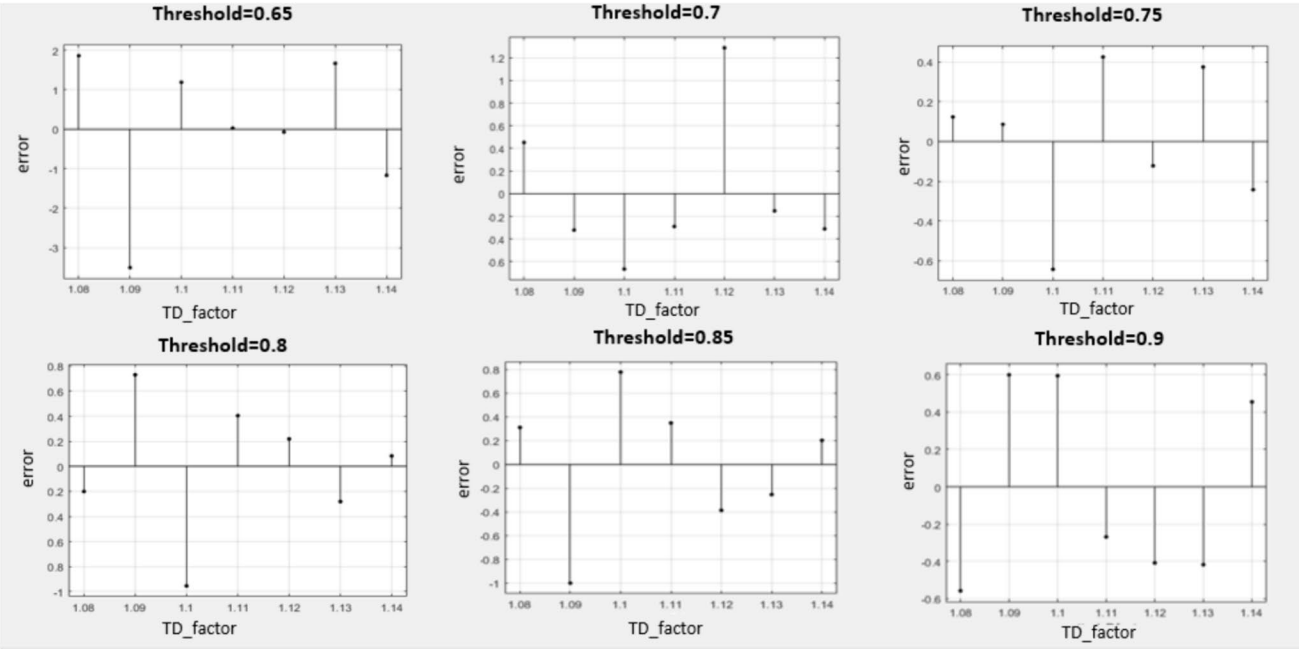

Fig. 12 Residual plot for the quadratic relationship between permeability reduction and TD_factor for different values of Threshold

with the best available tools. This study has explored the use of the LBM to simulate polymer gel injection in a 2D Berea sample, representing a realistic porous media. The time dependate behavior of polymer and x-linker solution which eventually forms the gel to blok pores has been considered through two key simulation parameters: TD_factor and Threshold.

Palabos software was utilized for the simulations, and the results pertaining to both the non-Newtonian fluid model and the flow in porous media were verified against Poiseuille flow and Darcy's law respectively. Various simulations were conducted to examine the impact of gelation parameters on altering the geometry of the 2D Berea sample and on the permeability reduction in the porous media. The result represent the capability of proposed methodology to model ormation of gel in pores, as the gel was mainly form in high permeable conduits, i.e. relatively larger pores. Key findings include:

- The capability of proposed methodology to model formation of gel in pores, as the gel was mainly form in high permeable conduits, i.e. relatively larger pores which is desireable for water shut-off treatment
- It was concluded that increasing the value of TD_factor, which is responsible for signifying the time-dependancy and increasing viscousity of fluid was resulted in blocking more pores, which shows the ability of proposed methodology to consider different peroperties for polymer gel.
- The study established a quadratic relationship between permeability reduction and the gelation parameters, specifically TD_factor and Threshold, demonstrating the predictive strength of the Lattice Boltzmann Method (LBM) in modeling polymer gel flow in porous media.
- It was observed that the TD_factor has a more substantial impact on permeability reduction than the Threshold, as indicated by the larger absolute value of the quadratic term coefficient. This suggests that TD_factor optimization could more effectively control gelation behavior.

In conclusion, the research demonstrates innovative use of the step-wise LBM in predicting the time-dependent behavior of non-Newtonian fluids within porous media, a promising tool for the design and optimization of water shutoff treatments in the petroleum industry. The research also outlines clear directions for future research, including the potential for refining the model by either considering the anisotropic porous media or incorporating calculations

Table 7 Coefficient and metrics for the quadratic relationship between permeability reduction, TD_factor, and Threshold

p00	p10	p01	p20	p11	p02	SSE	R-square	Adj R-sq	RMSE
− 7218	10,830	2715	− 4000	− 2011	− 255	47.24	0.99	0.99	1.15

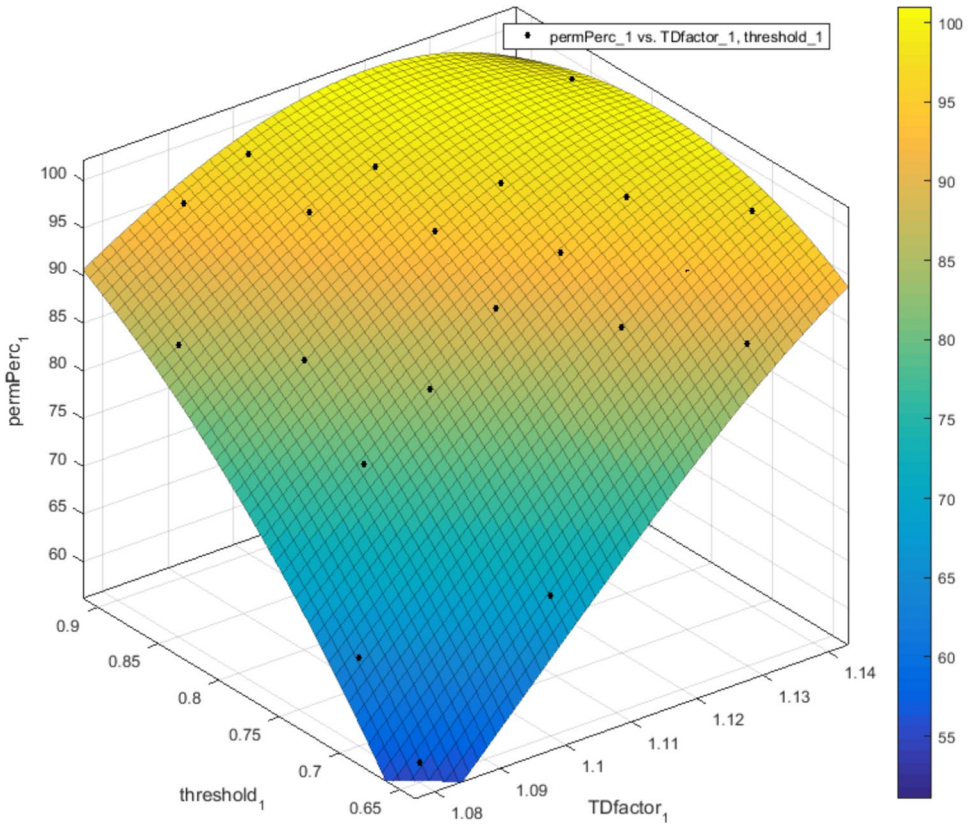

Fig. 13 Quadratic relationship between permeability reduction, threshold and TD_factor. the simulation results are represented as dots and the plane shows the predicted value for permeability reduction

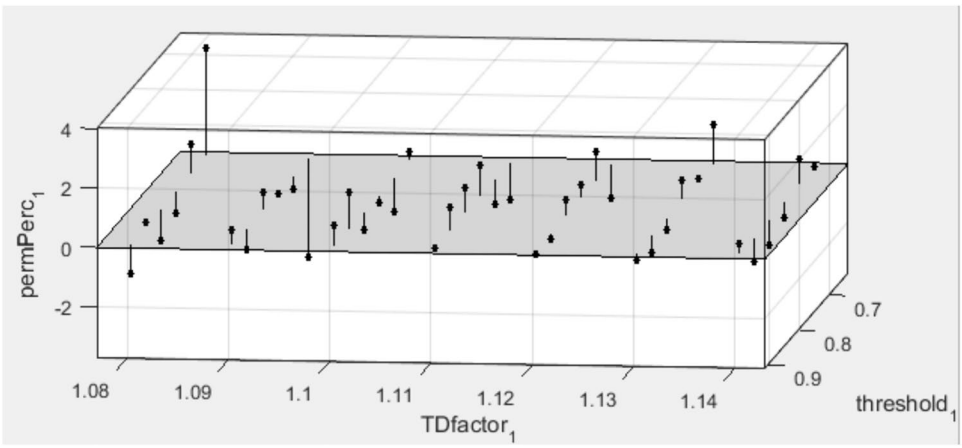

Fig. 14 Residual plot for the quadratic relationship between permeability reduction, threshold and TD_factor

for drag forces and the dynamic nature of gelation areas, thereby enhancing the accuracy of permeability control predictions.

Author contribution Elahe Kamel Targhi: conceptualization, methodology, software, coding, investigation, writing original draft, formal analysis. Mohammad Emami Niri: conceptualization, validation, resources, supervision, writing review & editing. Mohammad Reza Rasaei: conceptualization, validation, resources, supervision, writing review & editing. Pacelli L. J. Zitha: validation, supervision, writing review & editing.

Declarations

Conflict of interest The authors declare that they have no known competing financial interests or personal relationships that could have appeared to influence the work reported in this paper. On behalf of all the co-authors, the corresponding author states that there is no conflict of interest.

References

Adam S, Premnath KN (2019) Numerical investigation of the cascaded central moment lattice Boltzmann method for non-Newtonian fluid flows. J Non-Newton Fluid Mech 274:104188

Afrouzi HH, Ahmadian M, Moshfegh A, Toghraie D, Javadzadegan A (2019) Statistical analysis of pulsating non-Newtonian flow in a corrugated channel using Lattice-Boltzmann method. Phys A Stat Mech Appl 535:122486

Aharonov E, Rothman DH (1993) Non-Newtonian flow (through porous media): a Lattice-Boltzmann method. Geophys Res Lett 20(8):679–682

Al-Shajalee F, Arif M, Machale J, Verrall M, Almobarak M, Iglauer S, Wood C (2020) A multiscale investigation of cross-linked polymer gel injection in sandstone gas reservoirs: implications for water shutoff treatment. Energy Fuels 34(11):14046–14057

Anbar S, Thompson KE, Tyagi M (2019) The impact of compaction and sand migration on permeability and non-darcy coefficient from pore-scale simulations. Transp Porous Media 127(2):247–267

Ashrafizaadeh M, Bakhshaei H (2009) A comparison of non-Newtonian models for lattice Boltzmann blood flow simulations. Comput Math Appl 58(5):1045–1054

Bai B, Zhou J, Yin M (2015) A comprehensive review of polyacrylamide polymer gels for conformance control. Pet Explor Dev 42(4):525–532

Bhatnagar PL, Gross EP, Krook M (1954) A model for collision processes in gases. I. Small amplitude processes in charged and neutral one-component systems. Phys Rev 94(3):511

Bigdeli A, Delshad M (2023) Strategy for optimum chemical enhanced oil recovery field operation. J Resour Recovery. https://doi.org/10.52547/JRR.2208.1001

Bigdeli A, Thyne G, Ulyanov V (2023a) Low salinity water flooding (LSWF), can we move forward? the economic case. J Resour Recovery. https://doi.org/10.52547/JRR.2209.1002

Bigdeli A, von Hohendorff Filho JC and Schiozer DJ (2023) Effect of liquid-liquid subsea separation on production forecast considering integration of a deepwater reservoir and surface facility models. In: Society of petroleum engineers—SPE EuropEC—Europe energy conference featured at the 84th EAGE annual conference and exhibition, EURO 2023. https://doi.org/10.2118/214455-MS

Blunt MJ (2017) Multiphase flow in permeable media: a pore-scale perspective. Cambridge University Press, Cambridge

Boek ES, Chin J, Coveney PV (2003) Lattice Boltzmann simulation of the flow of non-Newtonian fluids in porous media. Int J Modern Phys B 17(01n02):99–102

Boek ES, Venturoli M (2010) Lattice-Boltzmann studies of fluid flow in porous media with realistic rock geometries. Comput Math Appl 59(7):2305–2314

Boyd J, Buick J, Green S (2006) A second-order accurate lattice Boltzmann non-Newtonian flow model. J Phys Math General 39(46):14241

Boyd J, Buick JM (2007) Comparison of Newtonian and non-Newtonian flows in a two-dimensional carotid artery model using the lattice Boltzmann method. Phys Med Biol 52(20):6215

Boyd J, Buick JM, Green S (2007) Analysis of the Casson and Carreau-Yasuda non-Newtonian blood models in steady and oscillatory flows using the lattice Boltzmann method. Phys Fluids 19(9):93103

Chen S, Doolen GD (1998) Lattice Boltzmann method for fluid flows. Annu Rev Fluid Mech 30(1):329–364

Chen Y-L, Cao X-D, Zhu K-Q (2009) A gray lattice Boltzmann model for power-law fluid and its application in the study of slip velocity at porous interface. J Non-Newton Fluid Mech 159(1–3):130–136

Chen Z, Shu C (2020) Simplified lattice Boltzmann method for non-Newtonian power-law fluid flows. Int J Numer Meth Fluids 92(1):38–54

Cristobal E and Riera P (2018) Viscoelastic fluid simulation with lattice-Boltzmann methods

Dong L, Yue X, Su Q, Qin W, Song W, Zhang D, Zhang Y (2016) Study on the plugging ability of polymer gel particle for the profile control in reservoir. J Dispers Sci Technol 37(1):34–40

Farnoush S, Manzari MT (2014) An investigation on the body force modeling in a lattice Boltzmann BGK simulation of generalized Newtonian fluids. Phys A Stat Mech Appl 415:315–332

Filho JC, von Victorino IRS, Bigdeli A, Schiozer DJ (2023) Application of water flooding and water alternative gas (WAG) flooding techniques in a carbonate reservoir: integration of reservoir and production systems for decision making. Braz J Pet Gas 17(4):179–202. https://doi.org/10.5419/BJPG2023-0012

Gabbanelli S, Drazer G, Koplik J (2005) Lattice Boltzmann method for non-Newtonian (power-law) fluids. Phys Rev E 72(4):46312

Ghoreishi SA, Sedaee B (2021) Numerical investigation of the most affecting parameters on foam flooding performance in carbonate naturally fractured reservoirs. Improv Oil Gas Recovery. https://doi.org/10.14800/IOGR.1194

Ginzburg I (2002) A free-surface lattice Boltzmann method for modelling the filling of expanding cavities by Bingham fluids. Philos Trans R Soc Lond Ser A Math Phys Eng Sci 360(1792):453–466

Giraud L, d'HumièRes D, Lallemand P (1997) A lattice-Boltzmann model for visco-elasticity. Int J Mod Phys C 8(04):805–815

Giraud L, d'Humieres D, Lallemand P (1998) A lattice Boltzmann model for Jeffreys viscoelastic fluid. EPL (europhys Lett) 42(6):625

Gokhale MY, Fernandes I (2017) Simulation of forced convection in non-Newtonian fluid through sandstones. Int J Comput Methods Eng Sci Mech 18(6):302–308

Golparvar A, Zhou Y, Wu K, Ma J, Yu Z (2018) A comprehensive review of pore scale modeling methodologies for multiphase flow in porous media. Adv Geo-Energy Res 2(4):418–440

Govindarajan SK (2019) An overview on extension and limitations of macroscopic Darcy's law for a single and multi-phase fluid flow through a porous medium. Int J Min Sci. https://doi.org/10.20431/2454-9460.0504001

Grasinger M, Overacker S, Brigham J (2018) Numerical investigation of the accuracy, stability, and efficiency of lattice Boltzmann methods in simulating non-Newtonian flow. Comput Fluids 166:253–274

Höök M, Hirsch R, Aleklett K (2009) Giant oil field decline rates and their influence on world oil production. Energy Policy 37(6):2262–2272

Hosseini-Nasab SM, Padalkar C, Battistutta E, Zitha PLJ (2016) Mechanistic modeling of the alkaline/surfactant/polymer flooding process under sub-optimum salinity conditions for enhanced oil recovery. Ind Eng Chem Res 55(24):6875–6888

Janssen MTG, Torres Mendez FA, Zitha PLJ (2020) Mechanistic modeling of water-alternating-gas injection and foam-assisted chemical flooding for enhanced oil recovery. Ind Eng Chem Res 59(8):3606–3616

Jia H, Pu W-F, Zhao J-Z, Liao R (2011) Experimental investigation of the novel phenol–formaldehyde cross-linking HPAM gel system: Based on the secondary cross-linking method of organic cross-linkers and its gelation performance study after flowing through porous media. Energy Fuels 25(2):727–736

Jiasheng LIU (2013) Improvement and test of water plugging technology for horizontal wells in heavy oil reservoirs with edge and bottom water. Contemp Chem Ind 42(3):290–293

KamelTarghi E, EmamiNiri M, ZithaP. LJ (2023) Design of Artificial Neural Network for predicting the reduction in permeability of porous media as a result of polymer gel injection. Geo Energy Sci Eng 227:211925. https://doi.org/10.1016/J.GEOEN.2023.211925

Kehrwald D (2005) Lattice Boltzmann simulation of shear-thinning fluids. J Stat Phys 121(1):223–237

Lallemand P, d'Humieres D, Luo L-S, Rubinstein R (2003) Theory of the lattice Boltzmann method: three-dimensional model for linear viscoelastic fluids. Phys Rev E 67(2):21203

Lashari ZA, Asadullah M, Ubedullah A, Memon, HU, Tunio AH (2014) Simulating the effects of water shut-off treatment by polymer gel injection. SPE/PAPG Pakistan Section Annual Technical Conference SPE-174708-MS. https://doi.org/10.2118/174708-MS

Latt J, Malaspinas O, Kontaxakis D, Parmigiani A, Lagrava D, Brogi F, Belgacem MB, Thorimbert Y, Leclaire S, Li S (2021) Palabos: parallel lattice Boltzmann solver. Comput Math Appl 81:334–350

Li Q, Hong N, Shi B, Chai Z (2014) Simulation of power-law fluid flows in two-dimensional square cavity using multi-relaxation-time lattice Boltzmann method. Commun Comput Phys 15(1):265–284

Liang X, Zhang H (2014) Research and appilcation of horiziontal well plugging water technology. Petrolchem Ind Appl 33(1):46–49

Liao J (2014) Gel treatment field application survey for water shut off in production wells

Malaspinas O, Courbebaisse G, Deville M (2007) Simulation of generalized Newtonian fluids with the lattice Boltzmann method. Int J Mod Phys C 18(12):1939–1949

Martys NS, Chen H (1996) Simulation of multicomponent fluids in complex three-dimensional geometries by the lattice Boltzmann method. Phys Rev E 53(1):743

McNamara GR, Zanetti G (1988) Use of the Boltzmann equation to simulate lattice-gas automata. Phys Rev Lett 61(20):2332

Mollahosseini A, Abdelrasoul A (2021) Molecular dynamics simulation for membrane separation and porous materials: a current state of art review. J Mol Graph Model 107:107947. https://doi.org/10.1016/J.JMGM.2021.107947

Mostafavi SA, Riahi S, Mavaddat M and Bigdeli A (2021) Best practices-design for scale reduction during produced water reinjection (PWRI). In: 82nd EAGE conference and exhibition 2021, vol 7(1), pp 5619–5623. https://doi.org/10.3997/2214-4609.202113312/CITE/REFWORKS

Olson JF, Rothman DH (1997) Two-fluid flow in sedimentary rock: simulation, transport and complexity. J Fluid Mech 341:343–370

Ouared R, Chopard B (2005) Lattice Boltzmann simulations of blood flow: non-Newtonian rheology and clotting processes. J Stat Phys 121(1):209–221

Ovaysi S, Piri M (2010) Direct pore-level modeling of incompressible fluid flow in porous media. J Comput Phys 229(19):7456–7476

Parmigiani A, Huber C, Bachmann O, Chopard B (2011) Pore-scale mass and reactant transport in multiphase porous media flows. J Fluid Mech 686:40–76

Pontrelli G, Ubertini S, Succi S (2009) The unstructured lattice Boltzmann method for non-Newtonian flows. J Stat Mech Theory Exp 2009(06):P06005

Rakotomalala N, Salin D, Watzky P (1996) Simulations of viscous flows of complex fluids with a Bhatnagar, Gross, and Krook lattice gas. Phys Fluids 8(11):3200–3202

Siddiki MN-A-A, Molla MM, Thohura S, Saha SC (2018) Lattice Boltzmann simulation of Non-Newtonian power-law fluid flows in a bifurcated channel. AIP Conf Proc 1980(1):40023

Sukop MC, Huang H, Lin CL, Deo MD, Oh K, Miller JD (2008) Distribution of multiphase fluids in porous media: comparison between lattice Boltzmann modeling and micro-x-ray tomography. Phys Rev E 77(2):26710

Sullivan SP, Gladden LF, Johns ML (2006) Simulation of power-law fluid flow through porous media using lattice Boltzmann techniques. J Non-Newton Fluid Mech 133(2–3):91–98

Sutera SP, Skalak R (1993) The history of Poiseuille's law. Annu Rev Fluid Mech 25(1):1–20

Sydansk RD, Romero-Zerón L (2011) Reservoir conformance improvement. Society of Petroleum Engineers Richardson, TX

Taha A, Amani M (2019) Overview of water shutoff operations in oil and gas wells; chemical and mechanical solutions. ChemEng 3(2):51

Tang GH, Wang SB, Ye PX, Tao WQ (2011) Bingham fluid simulation with the incompressible lattice Boltzmann model. J Non-Newton Fluid Mech 166(1–2):145–151

Veliyev EF, Aliyev AA, Guliyev VV and Naghiyeva NV (2019) Water shutoff using crosslinked polymer gels. In: Society of petroleum engineers—SPE annual caspian technical conference 2019, CTC 2019. https://doi.org/10.2118/198351-MS

Wang C-H, Ho J-R (2011) A lattice Boltzmann approach for the non-Newtonian effect in the blood flow. Comput Math Appl 62(1):75–86

Wang D, Bernsdorf J (2009) Lattice Boltzmann simulation of steady non-Newtonian blood flow in a 3D generic stenosis case. Comput Math Appl 58(5):1030–1034

Weiwei W, Shouli S, Zhouzhou W, Shuang D (2019) A universal modified MRT LBM for common non-Newtonian fluids and their applications. Mech Mater 139:103187

Wu W, Huang X, Yuan H, Xu F, Ma J (2017) A modified lattice boltzmann method for herschel-bulkley fluids. Rheol Acta 56(4):369–376

Yerramilli RC, Zitha PLJ, Yerramilli SS, Bedrikovetsky P (2015) A novel water-injectivity model and experimental validation with CT-scanned corefloods. SPE J 20(06):1200–1211. https://doi.org/10.2118/165194-PA

Yoshino M, Hotta Y, Hirozane T, Endo M (2007) A numerical method for incompressible non-Newtonian fluid flows based on the lattice Boltzmann method. J Non-Newton Fluid Mech 147(1–2):69–78

Zheng J, Wang Z, Ju Y, Tian Y, Jin Y, Chang W (2021) Visualization of water channeling and displacement diversion by polymer gel treatment in 3D printed heterogeneous porous media. J Petrol Sci Eng 198:108238

Zitha PLJ, Botermans CW, Jvd H, Vermolen FJ (2002) Control of flow through porous media using polymer gels. J Appl Phys 92(2):1143–1153

Zou Q and He X (1995) On pressure and velocity flow boundary conditions for the lattice Boltzmann BGK model. ArXiv Preprint Comp-Gas/9508001

Zou S, Yuan X-F, Yang X, Yi W, Xu X (2014) An integrated lattice Boltzmann and finite volume method for the simulation of viscoelastic fluid flows. J Non-Newton Fluid Mech 211:99–113